# Reduction in optical reflection at intermediate adhesive layer for mechanically stacked multi junction solar cells

**Toshiyuki Sameshima*, Yoshihiro Ogawa and Masahiko Hasumi**

*Electrical Engineering Department, Tokyo University of Agriculture and Technology, 2-24-16, Nakacho, Koganei, Tokyo 184-8588, Japan.*

*Corresponding author

DOI: 10.5185/amp.2018/409
www.vbripress.com/amp

## Abstract

Reduction of optical reflection loss at the intermediate region is discussed in three mechanical stacked samples: top Si and bottom Ge substrates, top GaAs and bottom Si substrates, and top GaP and bottom Si substrates using an epoxy-type adhesive with a reflective index of 1.47. Transparent conductive Indium gallium zinc oxide (IGZO) layers with a refractive index of 1.85 were used as antireflection layers. IGZO layers were formed on the bottom surface of the top substrate and the top surface of the bottom substrate of the three stacked samples with thicknesses of 188, 130, and 102 nm. The IGZO layers well decreased the optical reflectivity of the stacked samples. The IGZO layers provided high effective optical absorbency $A_{eff}$ of bottom substrates of 0.925, 0.943, and 0.931, respectively, for light wavelength regions for light in which the top substrates were transparent and the bottom substrates were opaque. High $A_{eff}$ maintained for the light incident angle between 0 to 50°. 

**Keywords:** Antireflection, optical interference, IGZO. multi-junction solar cell.

## Introduction

Semiconductor solar cells are important devices, which produce electrical power directly from sunlight [**1-3**]. To overcome the Shockley-Queisser limitation [**1**] of the conversion efficiency $E_{ff}$ of a single solar cell and realize a higher $E_{ff}$, a multi-junction solar cell has been proposed [**4-9**]. A combination of solar cells with different band gaps effectively absorb sunlight from ultraviolet to infrared wavelength regions. Solar cells ohmic-connected cooperatively increase the open circuit voltage $V_{oc}$. A three-junction solar cell InGaP/GaAs/Ge with $E_{ff}$ of 31.5% fabricated by the epitaxial crystalline growth method has been reported. Mechanically stacked multi-junction solar cells have also been reported [**10-13**]. The mechanical stacking method of individual solar cells allows a wide selection of semiconductor materials such as amorphous, polycrystalline, and organic semi-conductors as well as single-crystalline inorganic semiconductors. Moreover, this method makes it possible to fabricate large size solar cells. We have proposed a processing method of mechanically stacking semiconductor solar cells with a transparent conductive adhesive dispersed with indium-thin-oxide (ITO) conductive particles [**13, 14**]. A connecting resistivity lower than 1.0 $\Omega cm^2$ has been achieved. It was low enough to fabricate multi-junction solar cells with $E_{ff}$ higher than 30%. On the other hand, large difference in refractive indexes of semiconductor materials and adhesive causes high optical reflection, which reduces transmittance of light into the bottom cell. We propose conductive and transparent IGZO layers formed between the semiconductor substrates and intermediate adhesive to reduce optical reflection loss [**15**].

In this paper, we report the experimental demonstration of reduction of optical reflection loss using IGZO layers at the intermediate adhesive region at wavelength ranging from the visible to infrared region. We use three kinds of stacked samples: top crystalline Si and bottom crystalline Ge, top crystalline GaAs and bottom Si, and top crystalline GaP and bottom Si to discuss optical reflectivity properties. Two IGZO layers are used at the bottom interface of the top substrate and the top interface of the bottom substrate in the intermediate adhesive region. We demonstrate the decrease in the optical reflectivity of all the stacked samples with IGZO layers but not in the controlled stacked sample without IGZO layers. We report the effective optical absorbency $A_{eff}$ of the bottom substrate higher than 0.9 caused by IGZO anti-reflection effect. Moreover, we report calculation and experimental demonstration of effective reduction in optical reflection loss with different incident angles of light.

## Experimental

Four kinds of single-crystalline semiconductor substrates of 500-μm-thick p-type 10 Ωcm (100) Ge, 500-μm-thick n-type 17 Ωcm (100) Si, 500-μm-thick n-type 20 Ωcm (100) GaAs, and 500-μm-thick n-type 5 Ωcm (100) GaP were prepared to make stacked samples of Si/Ge, GaAs/Si, and Si/GaP. Our optical investigation focused in the wavelength region, in which the top substrate is transparent and the bottom substrate is opaque. The measurement of optical reflectivity spectra for Ge, Si, GaAs, and GaP substrates determined the wavelength region with the shortest wavelength $\lambda_1$ and the longest wavelength $\lambda_2$, as shown in **Table I**. IGZO films were formed on the semiconductor surfaces by radio-frequency Ar plasma sputtering at 2000 W with $In_{1.0}Ga_{1.2}Zn_{1.0}O_{1.4}$ as the target at room temperature. The thicknesses of the IGZO layer ($d_{ex}$) for 188 nm in stacked Si and Ge, 130 nm in stacked GaAs and Si, and as 102 nm in stacked GaP and Si, as listed in **Table I**. The IGZO layers formed on the semiconductor substrates were heated at 350ºC in air atmosphere for 1 h to increase resistivity to 0.056 Ωcm for preventing serious free carrier absorption in the infrared region in stacked Si and Ge. A transparent epoxy pre-polymer and hardener gels were prepared. 20-μm-diameter ITO particles were then dispersed at 6 wt% (1 vol%) in the gels. The adhesive with ITO particles was pasted on the surfaces of the bottom substrates. The top substrate was placed on the adhesive. The samples were then kept for 1.5 h at RT in 0.8 MPa $N_2$ atmosphere to solidify the epoxy adhesive. The connecting resistivity lower than 1.0 Ωcm was realized. Stacked samples were consequently fabricated with structures of Si/IGZO/ adhesive/IGZO/Ge, GaAs/IGZO/adhesive/IGZO/Si, and GaP/IGZO/adhesive/IGZO/Si. Moreover, samples with structures of Si/adhesive/Ge, GaAs/adhesive/Si, and GaP/adhesive/Si were also fabricated as the control samples. The optical reflectivity spectra of the stacked samples were measured using a spectrometer in the case of light illumination to the top surface of the samples.

Optical reflectivity spectra of the samples were also measured with integrated sphere equipment with incident angles ranging from 0 to 20º. Moreover, a homemade optical reflection measurement system with incident angle from 10 to 50º was also used, as shown in **Fig. 1**. Light of AM 1.5 was slant irradiated to the sample. A crystalline GaP wafer was placed as optical filter which cut light with photon energy higher than GaP band gap. Reflection light was detected by a two dimensional Si photodetector. The angles of incident and reflectance lights were coincidentally changed from 10 to 50º. Consequently, reflectance light was detected for wavelength between $\lambda_1$ and $\lambda_2$ for stacked GaP and Si sample.

## Calculation

A numerical calculation program of optical reflectivity spectra was developed to analyze experimental reflectivity spectra and $A_{eff}$ with data of the refractive index $n$ and extinction coefficient $k$ [**16, 17**]. The top and bottom substrates were thick enough to ignore the optical interference effect of incident incoherent light. The intermediate adhesive layer has a thickness of about 20 μm in reality. We also assumed that no optical interference effect occurred between the top and bottom adhesive surfaces. The Fresnel-type optical interference effect was calculated for the IGZO layer assuming a simple plain wave model [**18**]. The optical phase coupling results in an interface with a new reflectivity coefficient depending on the IGZO film thickness for both surfaces of the intermediate adhesive layer. A multiple reflections and transmission calculation system was prepared with different incident angles to obtain optical reflectivity The extinction coefficient $k$ also gives the reduction in light intensity by $\exp(-4\pi kx/\lambda)$ when light propagates for a distance of $x$ at $\lambda$. When the wavelength is located between $\lambda_1$ and $\lambda_2$, the top substrate is transparent and the bottom substrate is still opaque. The optical reflectivity of the sample is given by multiple reflection components between the three top interfaces as well as a component given by the top surface, as shown in **Fig. 2**. The reflectivity at second and third interfaces given by IGZO is therefore important to reduce the total reflectivity. To estimate optical reflection loss, the effective optical absorbency $A_{eff}$ was defined as

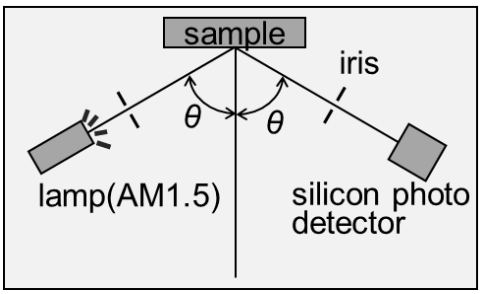


**Fig. 1.** Home-made optical reflection measurement system with incident angle from 10 to 50º.

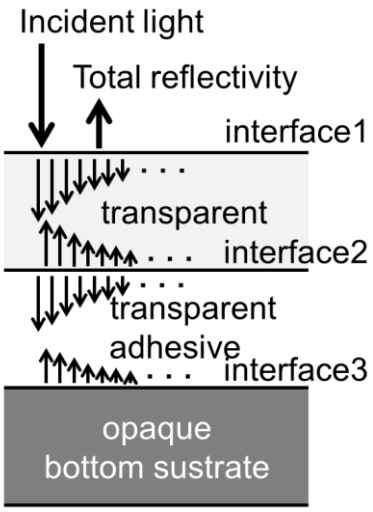


**Fig. 2.** Calculation illustrations of scalar-type multiple reflections and transmission with an incident angle of 0 between the three interfaces of air/top substrate, top substrate/adhesive, and adhesive/bottom substrate, and bottom substrate/air for wavelength between $\lambda_1$ and $\lambda_2$ ($\lambda_1<\lambda<\lambda_2$).

$$A_{eff} = \frac{\int_{\lambda_1}^{\lambda_2}\left[100 - R_s(\lambda)\right]d\lambda}{\int_{\lambda_1}^{\lambda_2}\left[100 - r(\lambda)\right]d\lambda} \quad , (1)$$

where $R_s(\lambda)$ is the optical reflectivity (%) of the sample at the wavelength $\lambda$, and $r(\lambda)$ is the reflectivity (%) at the top surface of an individual top substrate. The denominator is the integration of light incidence ratio into the top substrate between $\lambda_1$ and $\lambda_2$ because the top substrate was transparent between $\lambda_1$ and $\lambda_2$. The numerator is the integration of the optical absorption ratio of the sample between $\lambda_1$ and $\lambda_2$. Because the bottom substrate was opaque at wavelength shorter than $\lambda_2$, the numerator of eq. (1) depends on the reflectivity at the interface adhesive layer. $A_{eff}$ therefore gives the effective optical absorbency of the bottom substrate of incident light at the top substrate. The optical reflection loss ratio of the intermediate adhesive layer between $\lambda_1$ and $\lambda_2$ is therefore given by 1-$A_{eff}$. For sample fabrication, the thickness of the IGZO layer $d_{cal}$ was determined by the maximum calculated $A_{eff}$ in the case of the incident angle of 0°. The values of $d_{cal}$ were 183 nm in stacked Si and Ge, 130 nm in stacked GaAs and Si, and 102 nm in stacked GaP and Si, respectively.

**Table I**. Lists of materials for fabricating stacked samples, $\lambda_1$, $\lambda_2$, $\lambda_{eff}$, $d_{cal}$, and $d_{ex}$ in nm.

| Sample | $\lambda_1$ | $\lambda_2$ | $\lambda_{eff}$ | $d_{cal}$ | $d_{ex}$ |
|---|---|---|---|---|---|
| Si/Ge | 1150 | 1600 | 1356 | 183 | 188 |
| GaAs/Si | 902 | 1020 | 959 | 130 | 130 |
| GaP/Si | 568 | 1020 | 761 | 102 | 102 |

## Results and discussion

**Fig. 3** shows the optical reflectivity spectra of the samples with structures of (a) Si/IGZO/adhesive/IGZO/Ge and Si/adhesive/Ge, (b) GaAs/IGZO/adhesive/IGZO/Si and GaAs/adhesive/Si, and (c) GaP/IGZO/adhesive/IGZO/Si and GaP/adhesive/Si at the incident angle of 5°. The hatched areas show wavelength regions ranging from $\lambda_1$ to $\lambda_2$ given in **Table I** each figure, in which the top substrate is transparent and the bottom substrate is opaque. Light coming in the top surface can partially reflect at the intermediate adhesive region and comes back to the top surface. The optical reflectivity measurement at the top surface therefore gives the degree of optical reflection at the intermediate adhesive region. The sample with 188-nm-thick IGZO layers formed on the bottom surface of the Si substrate and the top surface of Ge substrate showed an optical reflectivity of 38.6% at 1150 nm. The optical reflectivity gradually decreased to 36.4% as the wavelength increased to 1600 nm. At a low optical reflectivity, it is clearly demonstrated that the IGZO layer showed the anti-reflection effect. Light was effectively transmitted from Si to Ge with no substantial light reflection at the intermediate adhesive region. On the other hand, the control sample, Si/adhesive/Ge, showed a

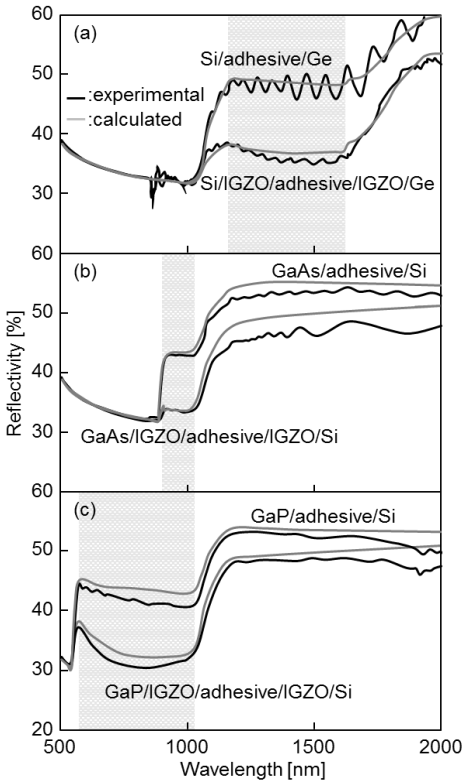


**Fig. 3.** Experimental and calculated optical reflectivity spectra of samples with structures of (a) Si/IGZO/adhesive/IGZO/Ge and Si/adhesive/Ge, (b) GaAs/IGZO/adhesive/IGZO/Si and GaAs/adhesive/Si, and (c) GaP/IGZO/ adhesive/IGZO/Si and GaP/adhesive/Si. The hatched areas show wavelength regions between $\lambda_1$ and $\lambda_2$ given in **Table I**.

high optical reflectivity between 46.7 and 50.2% at wavelengths ranging from 1150 to 1600 nm. The high optical reflectivity resulted from substantial reflections at the interfaces between Si and the adhesive and between the adhesive and Ge. **Fig. 3(a)** also shows the calculated optical reflectivity spectra of samples with structures of Si/188-nm-thick IGZO/adhesive/188-nm-thick IGZO/Ge and Si/adhesive/Ge. The calculated spectra showed characteristics similar to the experimental spectra over the wavelength region from 500 to 2000 including the region ranging from $\lambda_1$ (1150 nm) to $\lambda_2$ (1600 nm). The optical reflectivity of four cases of experimental and calculated spectra were almost the same. The good agreement among experimental and calculated values between 1150 and 1600 nm indicates that the optical reflectivity resulted from the effect multiple reflections among the top surface of crystalline Si, the Si/adhesive interface, and the adhesive/crystalline Ge interface.

The sample with 130-nm-thick IGZO layers formed on the bottom surface of the GaAs substrate and the top surface of the Si substrate showed optical reflectivities ranging from 33.4 to 33.9% between 902 and 1020 nm, as shown in **Fig. 3(b)**. These low optical reflectivities demonstrate that IGZO layer has the anti-reflection effect in the short wavelength region. Light effectively transmitted from GaAs to Si with no substantial light reflection at the intermediate adhesive region. On the

 

other hand, the control sample with GaAs/adhesive/Si showed high optical reflectivities between 40.1 and 42.3% at wavelengths ranging from 902 to 1020 nm. These high optical reflectivities were due to substantial optical reflection at the intermediate adhesive region. Calculated optical reflectivity spectra shown by gray curves agreed well with the experimental spectra of samples with the structures of GaAs/130-nm-thick IGZO/adhesive/130-nm-thick IGZO/Si and Si/adhesive/Ge at wavelengths ranging from 902 to 1020 nm. The good agreement among experimental and calculated values between 902 to 1020 nm indicates that optical reflectivity was due to the effect of multiple reflections among the top surface of crystalline GaAs, the GaAs/adhesive interface, and adhesive/crystalline Si interface.

The sample with 102-nm-thick IGZO layers formed on the bottom surface of the GaP substrate and the top surface of the Si substrate showed an optical reflectivity of 35.6% at 568 nm. The optical reflectivity decreased to 32.5% as the wavelength increased to 1020 nm, as shown in **Fig. 3(c)**. Light effectively transmitted from GaP to Si with no substantial light reflection at the intermediate adhesive region. On the other hand, the sample with GaP/adhesive/Si showed a high optical reflectivity between 44.4 and 41.0% at wavelengths ranging from 568 to 1020 nm. The high optical reflectivity was due to substantial optical reflection at the intermediate adhesive region. The calculated optical reflectivity spectra were similar to the experimental spectra for samples with the structures of GaP/102-nm-thick IGZO/adhesive/102-nm-thick IGZO/Si, and GaP/adhesive/Si. The calculation model of the anti-reflection effect of IGZO well explains the low experimental optical reflectivity from 568 to 1020 nm, while the calculated spectrum also explains the high experimental optical reflectivity with no anti-reflection effect in the control sample of GaP/adhesive/Si.

**Fig. 4** shows calculated $A_{eff}$ as a function of IGZO thickness for the three kinds of stacked samples with an incident angle of 0°. Experimental results are also plotted. $A_{eff}$ increased as the IGZO thickness increased for each sample. It peaked and then decreased as the IGZO thickness further increased. The zero thickness of IGZO was the control sample, which gave the lowest $A_{eff}$. They were 0.751, 0.811, and 0.796 for stacked samples of Si/Ge, GaAs/Si, and GaP and Si, respectively. The control samples had the highest optical reflection loss at the intermediate adhesive layer. $A_{eff}$ increased as the IGZO thickness increased and peaked at the IGZO thicknesses of 183, 130, and 102 nm in the cases of stacking Si and Ge, GaAs and Si, and GaP and Si, respectively. The peaks of $A_{eff}$ were higher than 0.9 in all the samples. The maximum $A_{eff}$ was 0.95 at d of 130 nm in the stacked GaAs and Si because the anti-reflection condition was effectively established in the narrow wavelength width between $\lambda_1$ (902 nm) and $\lambda_2$ (1020 nm). The large wavelength width of $\lambda_1$ and $\lambda_2$ results in low maximum $A_{eff}$, observed in stacked Si and Ge, because $\lambda_1$ (1150 nm) and $\lambda_2$ (1600 nm) are far different from $\lambda_{eff}$ (1356 nm) and the anti-reflection effect is weak at $\lambda_1$ and $\lambda_2$ under the best anti-reflection condition at $\lambda_{eff}$. $A_{eff}$ gradually decreased as the IGZO thickness further increased after reaching the peak because the anti-reflection condition shifted to wavelengths longer than $\lambda_{eff}$. The experimental $A_{eff}$ had similar high values to calculated $A_{eff}$. They were 0.925, 0.943, and 0.931 for samples with structures of Si/188-nm-thick IGZO/adhesive/188-nm-thick IGZO/Ge, GaAs / 130-nm-thick IGZO / adhesive / 130-nm-thick IGZO/Si, GaP/102-nm-thick IGZO/adhesive/102-nm-thick IGZO/Si, respectively.

**Fig. 5** shows experimental optical reflectivity spectra for the samples of GaP/102nm-IGZO/adhesive/102nm-IGZO/Si and GaP/adhesive/Si with incident angles of 0 and 20°. Similar reflectivity spectra were observed for incident angles between 0 and 20°. The sample of GaP/102nm-IGZO/adhesive/102nm-IGZO/Si had optical reflectivity ranging from 40 to 33% for wavelength between 568 and 1020 nm, where GaP was transparent and Si was opaque. On the other hand, high optical reflectivity ranging from 48 and 44% was observed for the sample of GaP/adhesive/Si. These results indicate that the 102-nm-thick IGZO layer give good anti-reflection condition.

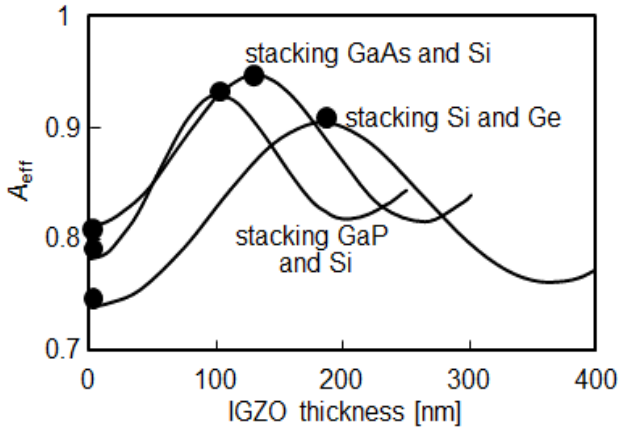


**Fig. 4.** Calculated $A_{eff}$ as a function of IGZO thickness for the three kinds of stacked samples with an incident angle of 0°. Experimental results are also plotted.

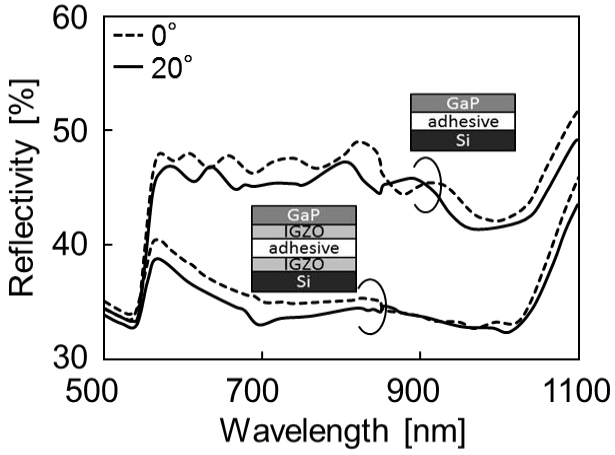


**Fig. 5.** Experimental optical reflectivity spectra for the samples of GaP/102nm-IGZO/adhesive/102nm-IGZO/Si and GaP/adhesive/Si with incident angles of 0 and 20°.

 

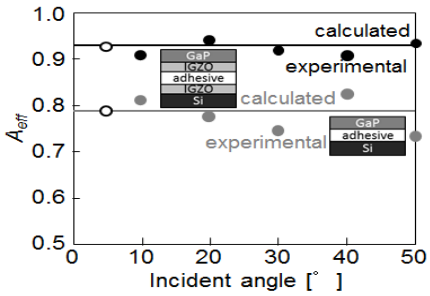


**Fig. 6.** Experimental $A_{eff}$ as a function of incident angle for the two samples measured by the system shown in **Fig. 1**

**Fig. 6** shows experimental $A_{eff}$ (solid circles) as a function of incident angle for the two samples measured by the system shown in **Fig. 1**. Experimental $A_{eff}$ obtained by the conventional spectrometer at the incident angle of 5° were shown by open circles. The calculated $A_{eff}$ values are also shown by solid curves. High $A_{eff}$ was observed for the sample of GaP/102nm-IGZO/adhesive/102nm-IGZO/Si structure. $A_{eff}$ ranged from 0.91 to 0.94 for incident angles between 10 and 50°. On the other hand, $A_{eff}$ ranged from 0.74 to 0.82 for the sample of GaP/adhesive/Si. The measurement results are consistent with the $A_{eff}$ values of 0.93 and 0.79 obtained from the spectrometer, respectively for the samples of GaP/102nm-IGZO/adhesive/102nm-IGZO/Si and GaP/adhesive/Si. For each sample, calculated $A_{eff}$ showed almost constant values for incident angles ranging from 0 to 50°. They showed good agreement with experimentally obtained values. High $A_{eff}$ is simply achieved by the formation of single layered anti-reflection IGZO films with appropriate film thickness.

## Conclusion

We demonstrated the reduction of optical reflection loss by IGZO-anti-reflection layers with a refractive index of 1.85 at the intermediate adhesive layer in the visible and infrared regions for mechanically stacked multi-junction solar cells. Three kinds of stacked samples with structures of Si/188-nm-thick IGZO/adhesive/188-nm-thick IGZO/Ge, GaAs/130-nm-thick IGZO/adhesive/130-nm-thick IGZO/Si, and GaP/102-nm-thick IGZO/adhesive/102-nm-thick IGZO/Si were fabricated using 6 wt% ITO particles dispersed in the epoxy adhesive with a refractive index of 1.47 by the sputtering method for IGZO formation. The Si/188-nm-thick IGZO/adhesive/188-nm-thick IGZO/Ge sample showed low optical reflectivities ranging from 38.6 to 36.4% at wavelengths ranging from 1150 to 1600 nm, where the top Si is transparent and the bottom Ge is opaque. The GaAs/130-nm-thick IGZO/adhesive/130-nm-thick IGZO/Si sample showed low optical reflectivities ranging from 33.4 to 33.9% at wavelengths ranging from 902 to 1020 nm. The GaP/102-nm-thick IGZO/adhesive/102-nm-thick IGZO/Si also showed low optical reflectivities ranging from 35.6 to 32.5% at wavelengths ranging from 568 to 1020 nm. Those values were lower than optical reflectivities of simple stacked samples with no IGZO layers.

These results experimentally demonstrated that the IGZO layer has the anti-reflection effect at the intermediate adhesive region. The three stacked samples with the IGZO anti-reflection layers described above gave high effective optical absorbency, $A_{eff}$, of the bottom substrates of 0.925, 0.943, and 0.931. Numerical analysis of the optical reflectivity spectra gave the best IGZO thicknesses of 183, 130, and 102 nm for the highest $A_{eff}$ for the three kinds of the samples. It successfully gave high $A_{eff}$ ranged from 0.91 to 0.94 for incident angles from 0 to 50°.

**Acknowledgements**

This work was supported by the New Energy and Industrial Technology Development Organization (NEDO) and Sameken Co., Ltd.

**References**

1. Shockley, W.; Queisser, H. J.; *J. Appl. Phys.*, **1961**, *32*, 510. **DOI:** 10.1063/1.1736034
2. Zhao, J.; Wang, A.; Green, M. A.; *Appl. Phys. Lett.*, **1998**, *73*, 1991. **DOI:** 10.1063/1.1122345
3. Shah, A. V.; Schade, H.; Vanecek, M.; Meier, J.; Vallat-Sauvain, E.; Wyrsch, N.; Kroll, U.; Droz, C.; Bailat, J.; *Photovoltaics*, **2004**, *12*, 113. **DOI:** 10.1002/pip.533
4. Sugiura, H.; Amano, C.; Yamamoto, A.; Yamaguchi, M; *Jpn. J. Appl. Phys.*, **1988**, *27*, 269. **DOI:** 10.1143/JJAP.27.269
5. Olson, J. M.; Kurtz, S. R.; Kibbler, A. E.; Faine, P; *Appl. Phys. Lett.*, **1990**, *56*, 623. **DOI:** 10.1063/1.102717
6. Takamoto, T.; Ikeda, E.; Kurita, H.; Ohmori, M.; Yamaguchi, M.; Yang, M. J.; *Jpn. J. Appl. Phys.*, **1997**, *36*, 6215. **DOI:** 10.1143/JJAP.36.6215
7. Yamaguchi, M.; *Physica E*, **2002**, *14*, 84. **DOI:** 10.1016/S1386-9477(02)00362-4
8. King, R. R.; Law, D. C.; Edmondson, K. M.; Fetzer, C. M.; Kinsey, G. S.; Yoon, H.; Sherif, R. A.; Karam, N. H.; *Appl. Phys. Lett.*, **2007**, *90*, 183516. **DOI:** 10.1063/1.2734507
9. Shahrjerdi, D.; Bedell, S.W.; Ebert, C.; Bayram, C.; Hekmatshoar, B.; Fogel, K.; Lauro, P.; Gaynes, M.; Gokmen, T.; Ott, A.; Sadana, D. K.; *Appl. Phys. Lett.*, **2012**, *100*, 053901. **DOI:** 10.1063/1.3681397
10. Mizuno, H.; Makita, K.; Matsubara, K.; *Appl. Phys. Lett.*, **2012**, *101*, 191111. **DOI:** 10.1063/1.4766339
11. Steiner, M. A.; Geisz, J. F.; Ward, J. S.; García, I.; Friedman, D. J.; King, R. R.; Chiu, R. T.; France, R. M.; Duda, A.; Olavarria, W. J.; Young, M.; Kurz, S. R.; *IEEE J. Photovoltaics*, **2016**, *6*, 358. **DOI:** 10.1109/JPHOTOV.2015.2494690
12. Wenger, S.; Seyrling, S.; Tiwari, A. N.; Grätzel, M.; *Appl. Phys. Lett.*, **2009**, *94*, 173508. **DOI:** 10.1063/1.3125432
13 Sameshima, T.; Takenezawa, J.; Hasumi, M.; Koida, T.; Kaneko, T.; Karasawa, M.; Kondo, M.; *Jpn. J. Appl. Phys.*, **2011**, *50*, 052301. **DOI:** 10.1143/JJAP.50.052301
14 Yoshidomi, S.; Furukawa, J.; Hasumi, M.; Sameshima, T.; *Energy Procedia*, **2014**, *60*, 116. **DOI:** 10.1016/j.egypro.2014.12.352
15. Sameshima, T.; Nimura, T.; Sugawara, T.; Ogawa, Y.; Yoshidomi, S.; Kimura, S.; Hasumi, M.; *Jpn. J. Appl. Phys.*, **2017**, *56*, 012602. **DOI:** 10.7567/JJAP.56.012602
16. Yoshidomi, S.; Kimura, S.; Hasumi, M.; Sameshima, T.; *Jpn. J. Appl. Phys.*, **2015**, *54*, 112301. **DOI:** 10.7567/JJAP.54.112301
17. Palik, E. D.; Handbook of Optical Constants of Solids; Academic Press: USA, **1985**. Subpart 2.
18. Sameshima, T.; Saitoh, K.; Sato, M.; Tajima, A.; Takashima, N.; *Jpn. J. Appl. Phys.*, **1997**, *36*, 1360. **DOI:** 10.1143/JJAP.36.L1360

 